Mid-frequency sound propagation through internal waves at short range with synoptic oceanographic observations

Daniel Rouseff, Dajun Tang, Kevin L. Williams, and Zhongkang Wang[a)]
Applied Physics Laboratory, College of Ocean and Fishery Sciences, University of Washington, 1013 NE 40th Street, Seattle, Washington 98105-6698
rouseff@apl.washington.edu, djtang@apl.washington.edu, williams@apl.washington.edu; zkwang@apl.washington.edu

James N. Moum
College of Oceanic and Atmospheric Sciences, Oregon State University, 104 COAS Administration Building, Corvallis, Oregon 97331-5503
jmoum@coas.oregonstate.edu

Abstract: Preliminary results are presented from an analysis of mid-frequency acoustic transmission data collected at range 550 m during the Shallow Water 2006 Experiment. The acoustic data were collected on a vertical array immediately before, during, and after the passage of a nonlinear internal wave on 18 August, 2006. Using oceanographic data collected at a nearby location, a plane-wave model for the nonlinear internal wave's position as a function of time is developed. Experimental results show a new acoustic path is generated as the internal wave passes above the acoustic source.

PACS numbers: 43.30.Ft, 43.30.Re, 43.30.Xm [WC]
Date Received: February 23, 2008 **Date Accepted:** June 18, 2008

1. Introduction

In shallow water, there is extensive ongoing research into the impact of nonlinear internal waves on low-frequency (<1 kHz) sound propagation.[1–4] Issues that have been studied include acoustic mode coupling and horizontal refraction of ray paths. By comparison, less attention has been devoted to the effect of internal waves in the mid-frequency (1–10 Hz) band.

During the Shallow Water 2006 Experiment (SW06), mid-frequency acoustic transmission data were collected over a continuous 7 h period at range 550 m. The relatively short range was deemed desirable for isolating the effects of shallow water internal waves on acoustic propagation. At the SW06 site, both linear and nonlinear internal waves were potentially important. Linear internal waves often are modeled as a background random process introducing small changes in the sound speed that cause fluctuations in the acoustic field. At range 550 m, mid-frequency transmissions between 1 and 10 kHz were thought to span the transition between the regimes where classical weak- and strong-scattering theories for random media would apply.[5] Nonlinear internal waves are often modeled as a more event-like process causing strong, localized changes in the sound speed. Packets of nonlinear internal waves are not unusual and it was anticipated that a 550 m acoustic path might permit individual waves in the packet to be isolated.

This paper describes an initial analysis of acoustic data collected immediately before, during, and after the passage of a nonlinear internal wave. The results show that new acoustic paths are generated and that these new paths are particularly strong as the nonlinear internal wave passes above the acoustic source.

[a)]Permanent affiliation: Hangzhou Applied Acoustics Research Institute, 96 Huaxing Road, Hangzhou, China.

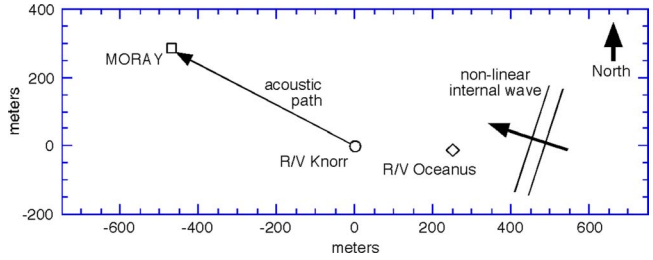

Fig. 1. (Color online) Experiment geometry. Acoustic source deployed off the stern of the R/V KNORR with transmitted signals measured 550 m away on MORAY vertical array. Oceanographic data were collected on R/V OCEANUS while a nonlinear internal wave passed.

2. Configuration of experiment

The SW06 experiment was performed in summer 2006 over the continental shelf of New Jersey, USA. The present analysis concentrates on data collected on 18 August in water nominally 80 m deep. When nonlinear internal waves were absent, the surface mixed layer extended to nominal depth 20 m.

The acoustic transmitter, an ITC-2015 (International Transducer Corporation) transducer, was positioned at 39 01.3152 N, 73 01.9364 W off the stern of the R/V KNORR. Deployment depth was 40 m to keep the transmitter below a thin layer of warm, salty water that was present that day at depth 30 m. Of present interest are linear frequency-modulated (LFM) chirp signals 20 ms in duration. The chirps spanned the 1.5–10.5 kHz frequency band with a raised cosine window and 10 percent taper. Transmissions were repeated approximately every 19 s.

The signals were recorded at range 550 m using the MORAY moored receiving system.[6] The system had two four-element vertical subarrays with the top four elements at depths 25.0, 25.2, 25.5, and 26.4 m, and the bottom four at 50.0, 50.2, 50.5, and 51.4 m. The data were stored at the array but a two-way radio frequency (rf) link permitted communication between MORAY and the R/V KNORR. The rf link was useful for adjusting amplifier gains, evaluating samples of the collected data, and assessing overall data quality.

While the acoustic data were being collected, investigators onboard the R/V OCEANUS collected oceanographic data (Fig. 1). At 20:53 Coordinated Universal Time (UTC), the R/V OCEANUS was positioned 250 m east of the R/V KNORR as a nonlinear internal wave first approached and then passed the two ships. The wave subsequently passed MORAY. X-band radar measurements estimated the bearing of the wave. Additional measurements included the water's temperature, salinity, density, and turbulence dissipation rate using the Chameleon turbulence profiler.[7] Two acoustic Doppler current profilers (ADCPs) were deployed to obtain vertical profiles of currents. A 120 kHz echosounder acoustically imaged the flow field.

3. Results

To understand the sequence of acoustic arrivals during quiescent periods when nonlinear internal waves were absent, the eigenrays from the source to different elements in the receiving array were calculated. The simulations assumed a range-independent environment and used three sound speed profiles collected from the R/V KNORR over a quiescent 4 h period. The simulations suggested that the direct acoustic path to the receiver at a depth of 50 m was the most sensitive to the details of the sound speed profile; depending on the particular profile, the direct path might or might not fragment into multiple direct arrivals. The fragmented direct path might arrive before or after the path that bounced off the sea surface. Furthermore, the direct path might be stronger or weaker than the surface bounce path. The acoustic ray that was launched at a downward angle and bounced once off the seabed, however, was strong and stable and insensitive to the particular sound speed profile used in the simulation.

Figure 2 shows a typical result from an acoustic transmission during a quiescent period. An LFM chirp signal measured at 50 m depth and 550 m range was matched filtered

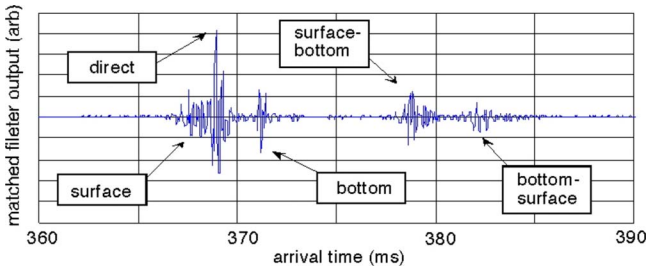

Fig. 2. (Color online) Typical acoustic arrival structure during quiescent period. Data collected on an array element at 50 m depth and 550 m range. Shown is the matched filter output where the various arrival paths are indicated.

yielding the arrival pattern for the different acoustic paths. The figure identifies the strongest direct path as well as four others: the sea surface bounce path, the bottom bounce path that reflected off the seabed, the surface-bottom bounce path and the bottom-surface path.

Figure 3 shows the fluid velocity measured from the R/V OCEANUS immediately before, during, and after the passage of nonlinear internal wave. Specifically, the vertical component of fluid velocity is mapped as a function of depth and time as measured by the ADCP. Isopycnals are superimposed. The maximum internal wave displacement is approximately 10 m and occurs at 21:14 UTC.

The oceanographic data collected on the R/V OCEANUS can be used to construct a simple model for the internal wave. When the internal wave was in the vicinity of the R/V OCEANUS, X-band radar measurements indicated the wave's bearing as 288 deg (Fig. 1) and its speed as 0.89 m/s. As an initial model, wavefront curvature is neglected and the internal wave is treated locally as a plane wave. The plane wave assumption, together with the known speed and direction of the wave, permits measurements made at the R/V OCEANUS to be propagated to other locations. Referring to the geometry in Fig. 1, the peak internal wave displacement observed on the R/V OCEANUS at 21:14 UTC will have propagated to the R/V KNORR at 21:18:30 UTC and to the MORAY at 21:28:31. The peak internal wave displacement, consequently, will lie somewhere between the acoustic transmitter and receiver for 10 min.

Figure 4 is a waterfall plot showing how the acoustic arrival structure measured at 50 m depth changes in time. The matched filter output is plotted for 100 consecutive LFM chirps with a gap of 18–20 s between transmissions. The 32 min of data include the periods immediately before, during, and after the passage of the internal wave. The superimposed horizontal lines bracket the time when the peak internal wave displacement, as calculated in the previous paragraph, is expected to pass between the acoustic source and receiver. The gross shifts in arrival time are due to relative motion between the source and the moored receiver. The bottom, bottom-surface, and surface-bottom bounce paths are labeled.

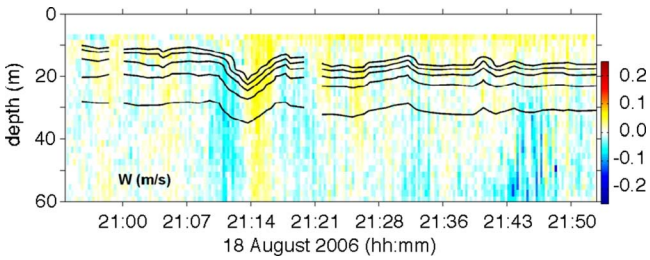

Fig. 3. (Color online) Sample oceanographic result showing vertical component of fluid velocity as measured on R/V OCEANUS. Contours of isopycnals are plotted over the color image. Peak isopycnal displacement from a nonlinear internal wave occurs at 21:14 UTC.

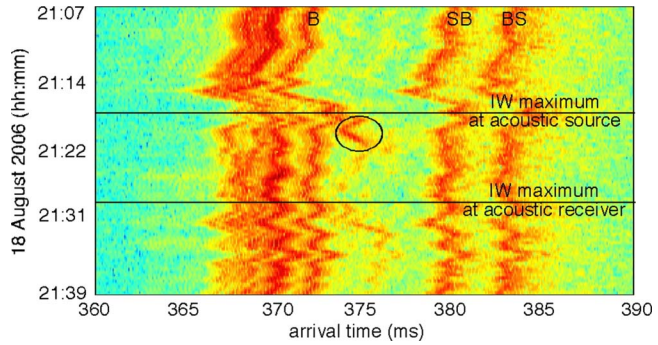

Fig. 4. (Color online) Time evolving acoustic arrival structure as the nonlinear internal wave in Fig. 3 enters the acoustic propagation path. The bottom, bottom-surface, and surface-bottom bounce paths are labeled. New acoustic path (circled) is generated as the internal wave passes above the acoustic source. Red-green-blue color scale has 50 dB dynamic range.

Similar arrival structures were observed on the other three elements in the bottom sub array. On each element, the bottom, bottom-surface, and surface-bottom bounce paths were strong and stable. Using the arrival times for a particular transmission as measured on each of the four array elements as input to a least-squares estimator, the arrival angle for a particular acoustic path could be estimated. Without correcting for array motion, the bottom bounce path had an average arrival angle of 8.4 deg relative to horizontal.

The most striking feature of Fig. 4 is the apparent generation of a new acoustic path as the internal wave passes above the acoustic source. The new path, circled in the figure as it appears, splits from the bottom bounce. At 21:21:13 UTC, approximately 3 min after the peak internal wave displacement has passed the acoustic source, the new path is at its strongest and its intensity exceeds the bottom bounce. Its arrival angle at 21:21:13 UTC is 12° and so steeper than the bottom-bounce path that precedes it. As the internal wave continues to move away from the acoustic source, the arrival angle for the new path continues to steepen but its intensity fades. It should be noted that a similar analysis was performed using the four elements in the upper sub array. On the upper sub array, whose shallowest element was at a depth of 25.0 m, the splitting of the bottom-bounce path was not observed as the internal wave passed.

A hypothesis is developed for the observed new ray. The passing internal wave depresses the mixed layer and hence the sound speed profile. Since the acoustic source is below the mixed layer, an upward-launched acoustic ray will be refracted downward by the passing internal wave. The refracted ray passes through an upper turning point and then strikes the bottom further down range than the original bottom-bounce path. After reflection, this new path arrives at the receiving array at a steeper angle than the unperturbed original bottom bounce.

4. Concluding remarks

Future work will include a more extensive data analysis together with numerical modeling. A complicating factor in developing a model is that the experiment was performed in a region where new individual internal waves were spawned rapidly.[8] Possible evidence for new internal waves is in Fig. 4 where a possible new acoustic arrival is apparent after the internal wave has passed the acoustic receiver at 21:28:31 UTC. Consequently, the simple plane-wave model for the internal waves used in the present work may prove inadequate for some calculations. To develop a more complete oceanographic model, temperature data collected on the MORAY acoustic array will be integrated into the analysis. A previously developed[9] ray tracing code valid for range-dependent media will then be applied in an attempt to reproduce and better understand the ray path generation observed in the data.

Acknowledgments

This work was supported by the Office of Naval Research.

References and links

[1]J. X. Zhou, X. Z. Zhang, and P. H. Rogers, "Resonant interaction of sound waves with internal solitons in the coastal zone," J. Acoust. Soc. Am. **90**, 2042–2054 (1991).
[2]R. H. Headrick, J. F. Lynch, J. N. Kemp, A. E. Newhall, K. von der Heydt, J. Apel, M. Badiey, C.-S. Chiu, S. Finette, M. Orr, B. Pasewark, A. Turgot, S. Wolf, and D. Tielbuerger, "Acoustic normal mode fluctuation statistics in the 1995 SWARM internal wave scattering experiment," J. Acoust. Soc. Am. **107**, 201–220 (2000).
[3]M. Badiey, Y. Mu, J. Lynch, J. Apel, and S. Wolf, "Temporal and azimuthal dependence of sound propagation in shallow water with internal waves," IEEE J. Ocean. Eng. **27**, 117–129 (2002).
[4]M. Badiey, B. G. Katsnelson, J. F. Lynch, S. Pereselkov, and W. L. Siegmann, "Measurement and modeling of three-dimensional sound intensity variations due to shallow-water internal waves," J. Acoust. Soc. Am. **117**, 613–625 (2005).
[5]B. J. Uscinski, *Elements of Wave Propagation in Random Media* (McGraw–Hill, New York, 1977), pp. 69–77.
[6]P. H. Dahl, J. W. Choi, N. J. Williams, and H. C. Graber, "Field measurements and modeling of attenuation from near-surface bubbles for frequencies 1–20 kHz," J. Acoust. Soc. Am. **124**, EL163–EL169 (2008).
[7]J. N. Moum, M. C. Gregg, R. C. Lien, and M. E. Carr, "Comparison of turbulence kinetic-energy dissipation rate estimates from two ocean microstructure profilers," J. Atmos. Ocean. Technol. **12**, 346–366 (1995).
[8]E. L. Shroyer, J. N. Moum, and J. D. Nash, "Observations of polarity reversal in shoaling non-linear internal waves," J. Phys. Oceanogr. , in press (2008).
[9]F. S. Henyey, D. Tang, K. L. Williams, R.-C. Lien, K. M. Becker, R. L. Culver, P. C. Gabel, J. E. Lyons, and T. C. Weber, "Effect of non-linear internal waves on mid-frequency acoustic propagation on the continental shelf," J. Acoust. Soc. Am. **119**, 3345 (2006).